

## Can a Small Number of Pedestrian Impact Scenarios Represent the Range of Real-world Pedestrian Injuries?

Guibing Li, Dietmar Otte, Jikuang Yang, Ciaran Simms

**Abstract** The purpose of this study is to evaluate the predictive capability of a virtual test system (VTS) proposed for vehicle front assessment of pedestrian injury risk. The VTS accounts for a broad range of impact scenarios in pedestrian accidents and the assessment is done using recent pedestrian accident data. Firstly, simulation test samples (STS) accounting for the broad range of vehicle impact speed, pedestrian height and gait stance in real world impact scenarios were developed based on different sets of multibody vehicle-to-pedestrian impact simulations. Then a sedan and a van model were tested using the defined STSs. The AIS2+ injuries predicted from these STSs for each vehicle model were weighted by the involving proportion of each impact scenario observed from German In-Depth Accident Study (GIDAS) pedestrian accident data via a defined Injury Weighting System (IWS). The injury predictive capability of the VTSs using different STS sample sizes and the corresponding IWS was evaluated by comparing the predicted AIS 2+ injury rate and distribution of AIS 2+ injuries as a function of pedestrian body region and height, vehicle class and impact speed with that observed from the GIDAS data. The results indicate that the proposed VTS using a STS of about 120 cases is broadly capable of predicting the AIS 2+ injury rate and distribution of pedestrian AIS 2+ injuries observed from the real-world accidents when the same vehicle class distribution as the accident data is employed. The VTS can be considered as an effective approach for assessing pedestrian safety performance of vehicle front designs at the generalised level.

**Keywords** multibody simulation, pedestrian impact scenarios, pedestrian injuries, virtual test system,

### I. INTRODUCTION

Pedestrians are vulnerable road users. Each year more than 1.17 million people are killed worldwide in road traffic accidents, and about 65% of injuries are to pedestrians [1]. The design of a vehicle front has significant effects on pedestrian injury risk in vehicle-to-pedestrian collisions [2]. As this has become recognised, vehicle front design has changed dramatically during the last two decades, but current vehicle designs remain aggressive to pedestrians in road traffic accidents [1]. An optimised vehicle front design for pedestrian protection is therefore an important goal.

Subsystem impactor tests, widely used in New Car Assessment Programmes (NCAPs) and in legislative tests to evaluate vehicle front design for pedestrian protection [3-5], are the main driver improving vehicle designs for pedestrian protection in the automobile industry. However, the broad range of impact scenarios in real-world pedestrian accidents is not accounted for in the subsystem impactor tests [3-5], yet pedestrian injury outcome is strongly dependent on the initial impact conditions [6-8]. Therefore, vehicle front optimisation for pedestrian protection must consider the broad range of impact scenarios and their actual distributions in real-world pedestrian accidents. Given the cost of physical testing, a computer-based approach is a practical optimisation approach, where a broad range of impact scenarios can be considered in a cost effective manner.

Accordingly, the authors recently proposed a Virtual Test System (VTS) to assess vehicle safety performance for pedestrian protection considering a broad range of impact configurations and their actual distributions observed from accident data [9]. The proposed VTS has two main parts: a Simulation Test Sample (STS) based on 1300 MADYMO multibody vehicle-to-pedestrian impact simulations accounting for the range of vehicle impact speeds, pedestrian heights and pedestrian gait stances to represent real world impact configurations and an Injury Weighting System (IWS) based on distributions of these impact parameters in accidents to

Guibing Li is a PhD student in Bioengineering at Trinity College Dublin in Ireland (Tel: +353 0 873922745, E-mail: guli@tcd.ie). Dietmar Otte is Prof. of accident analysis in the Accident Research Unit, Medical University of Hannover in Germany. Jikuang Yang is Prof. of Bioengineering in the Department of Applied Mechanics at Chalmers University of Technology in Sweden. Ciaran Simms is Prof. of Bioengineering in the Department of Mechanical and Manufacturing Engineering at Trinity College Dublin in Ireland.

appropriately weight the predicted injuries in the STS. The injury predictive capability of this VTS was evaluated by comparing the distributions of predicted AIS 2+ (Abbreviated Injury Scale-AIS, AIS 2+ means level 2 and plus) injuries as different pedestrian body regions and heights, as well as vehicle classes and impact speeds with that observed from the Pedestrian Crash Data Study (PCDS) database (1994-1998) [9]. The evaluation results showed good matches between the predicted AIS 2+ injury distributions and that from the PCDS database [9]. However this VTS has quite a large STS (N=1300) and was evaluated by comparison to accident database where the accident cases (N=552) were captured more than 15 years ago in 6 US cities [9].

Therefore, the purpose of this study is to investigate the effects of the STS size (number of impact scenarios) on the resulting injury predictive capability and to do this using up-to-date (2000-2015) pedestrian accident data from the German In-Depth Accident Study (GIDAS). The VTS will provide basic knowledge on which impact configurations should be considered in our future vehicle front optimization for pedestrian protection, where a large number of vehicle front designs will be evaluated.

## II. METHODS

### *Simulation test sample (STS)*

Details for the STS approach are available in [9]. Briefly, The STS is a set of impact configurations representing pedestrians struck from the side by a vehicle, designed to account for variations in vehicle impact speed, pedestrian height and pedestrian gait [2]. To control the computing time the STS was developed by applying discrete values for each input parameter. STSs of different sizes were defined based on varying the number of discrete cases in each group for impact speed, pedestrian height and gait stance, similar to [9]. However, in [9] 1300 cases were considered, while in this paper smaller sets were assessed. The pedestrian accident data captured during the period of 2000-2015 were extracted from the GIDAS database [10] as the inputs for the STS and the IWS.

TABLE I  
RANGES, MEAN VALUES AND INVOLVING PROPORTIONS ( $p_s$ )  
OF IMPACT SPEED IN GIDAS FOR DIFFERENT DISCRETE GROUPS

	Group	1	2	3	4	5	6	7	8	9	10	11	12
12 bins	Range	16-	21-	26-	31-	36-	41-	46-	51-	56-	61-	66-	71-
	(km/h)	20	25	30	35	40	45	50	55	60	65	70	75
	Mean	18	23	28	33	39	43	48	54	59	64	68	73
	$p_s$ (%)	18.0	15.8	16.6	13.0	12.1	9.5	7.6	2.0	2.3	1.9	0.7	0.7
9 bins	Range	16-	23-	30-	36-	44-	50-	56-	63-	70-			
	(km/h)	22	29	35	43	49	55	62	69	75			
	Mean	19	26	32	40	46	52	59	65	73			
	$p_s$ (%)	23.0	18.0	22.3	16.9	9.7	4.6	2.5	2.3	0.8			
6 bins	Range	16-	26-	36-	46-	56-	66-						
	(km/h)	25	35	45	55	65	75						
	Mean	21	31	41	50	61	70						
	$p_s$ (%)	33.7	29.5	21.6	9.6	4.2	1.4						
3 bins	Range	16-	36-	56-									
	(km/h)	35	55	75									
	Mean	26	43	63									
	$p_s$ (%)	63.2	31.2	5.6									

The ranges, mean values and involving proportions ( $p_s$ ) of the impact speed in GIDAS for different discrete groups are shown in Table I. In total four sets were chosen to form STSs of different sizes (12, 9, 6 and 3 cases). The selection of the impact speed range (16-75 km/h) is based on the fact that about 85% of AIS 2-6 injuries observed in the GIDAS data were caused by accidents within this speed range. Similarly Table II shows the ranges, mean values and involving proportions ( $p_h$ ) of pedestrian height in GIDAS and the heights of the representing multi-body pedestrian models for different discrete groups. In total four sets of discrete pedestrian heights were selected to form STSs of different sizes (10, 7, 5 and 3 cases). The choice of the height

groups was based on the availability of the MADYMO pedestrian models [11], including released models and scalable models, see Figure 1. In the simulations, pedestrian models similar to the mean sizes of the selected pedestrian height groups were used (Table II).

TABLE II  
RANGES, MEAN VALUES AND PROPORTIONS ( $P_H$ ) OF PEDESTRIAN HEIGHT IN GIDAS AND HEIGHTS OF THE REPRESENTING MULTI-BODY MODELS FOR DIFFERENT DISCRETE GROUPS.

	Group	1	2	3	4	5	6	7	8	9	10
10 bins	Range (cm)	<110	110-139	140-157	158-162	163-167	168-172	173-177	178-182	183-187	>187
	Mean	102	126	151	160	165	170	175	180	186	192
	Model	95	117	153	160	165	170	174	180	185	191
	$p_h$ (%)	3.6	11.1	16.9	15.7	11.4	15.7	13.0	6.8	3.6	2.2
7 bins	Range (cm)	<140	140-157	158-162	163-167	168-172	173-177	>177			
	Mean	120	151	160	165	170	175	183			
	Model	117	153	160	165	170	174	185			
	$p_h$ (%)	14.7	16.9	15.7	11.4	15.7	13.0	12.5			
5 bins	Range (cm)	<140	140-157	158-170	171-177	>177					
	Mean	120	151	164	174	185					
	Model	117	153	165	174	185					
	$p_h$ (%)	14.7	16.9	37.2	18.7	12.5					
3 bins	Range (cm)	<158	158-177	>177							
	Mean	130	168	185							
	Model	117	170	185							
	$p_h$ (%)	31.6	55.9	12.5							

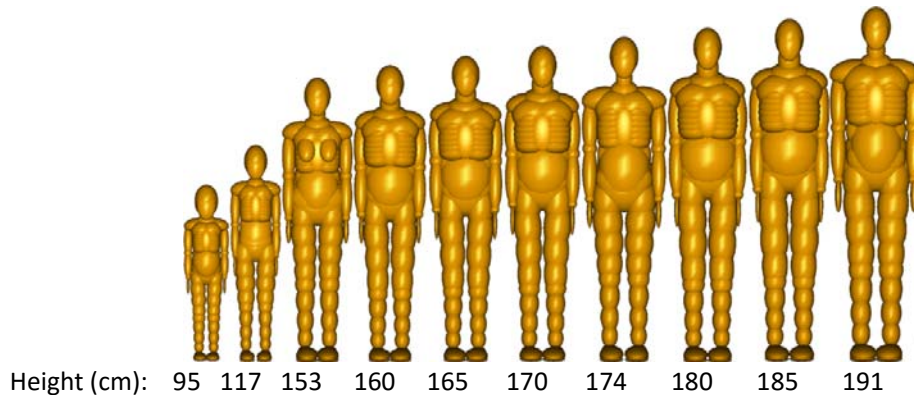


Fig. 1. The 10 MADYMO pedestrian models corresponding to the sizes in Table II [11].

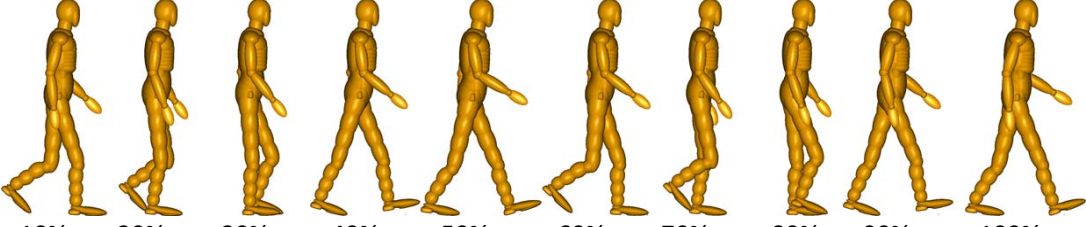
Discrete groups for pedestrian gait stance were also defined by using all or a part of the 10 gait stances proposed by [12] (10, 6, 4, 2 and 1 gait cases, see Table III). The choice of the pedestrian gait stance groups was based on the effects of gait stance on pedestrian leg [6] and head [7-8] kinematics and injuries. A uniform distribution was assumed for pedestrian gait stance since data for pedestrian gait stance is not available in accident data and all gait stances are considered equally likely.

A STS can then be defined by the discrete groups of impact speed, pedestrian height and gait stance selected from the above Tables (I-III), and the size of the STS is the product of the numbers in each discrete group for these three impact parameters, i.e. the size for a STS using nine impact speeds, seven pedestrian heights and six gait stances is 378 ( $9 \times 7 \times 6$ ). In total 35 STS candidates were developed based on different selections of impact parameters, which are the basic element of a VTS (see Table A.I (Appendix)), where the VTSs were named as the format VTS-No. speed-No. height-No. gait/No. scenarios, i.e. VTS-12-7-10/840 means that twelve impact

speeds, seven pedestrian heights and ten gait stances were used in the STS of 840 (12\*7\*10) impact configurations.

TABLE III  
PEDESTRIAN GAIT STANCES [12] AND THE ESTIMATED PROPORTIONS ( $P_g$ ) FOR DIFFERENT DISCRETE GROUPS.

	Group	1	2	3	4	5	6	7	8	9	10
10 bins	Gait	10%	20%	30%	40%	50%	60%	70%	80%	90%	100%
	$p_g$ (%)	10	10	10	10	10	10	10	10	10	10
6 bins	Range	10%	20%-30%	40%-50%	60%	70%-80%	90%-100%				
	Gait	10%	30%	50%	60%	80%	100%				
	$p_g$ (%)	10	20	20	10	20	20				
4 bins	Range	20%-30%	40%-60%	70%-80%	90%-100%						
	Gait	30%	50%	80%	100%						
	$p_g$ (%)	20	30	20	30						
2 bins	Range	20%-60%	70%-100%								
	Gait	50%	100%								
	$p_g$ (%)	50	50								
1 bin	Range	10%-100%									
	Gait	50%									
	$p_g$ (%)	100									

10% 20% 30% 40% 50% 60% 70% 80% 90% 100%

### Vehicle-to-pedestrian impact simulation

Multi-body front models of a sedan and a van (Figure 2) based on Ford Focus (2012) and Nissan Caravan E25 respectively [13] were used for modelling vehicles involved in the GIDAS accidents to evaluate the predictive ability of the proposed VTs (Table A.I). The selection of these vehicle models was based on the main vehicle classes and geometries involved in the GIDAS (93% cases for sedans and 6% cases for vans [10]). The SUV cases are not considered here since these only account for 1% GIDAS pedestrian accidents [10]. The geometries of the vehicle models were from real world car shapes [13]. Then these vehicle front models were tested using the STS, respectively.

It was assumed that the same contact definitions for the different vehicle regions could be applied to the sedan and van model in the STS. Force/deformation curves for the bumper and bonnet leading edge were extracted from impactor test data [14], while the bonnet and windscreen stiffness were sourced from the test data of [15]. For the pedestrian-ground interaction, only the pedestrian contact characteristics were used and the ground was modelled as a rigid surface [13] since no validated contact model is available yet. For the contact friction coefficient, 0.3 for the vehicle-to-pedestrian contacts and 0.58 for the pedestrian-to-ground interaction was defined as in previous studies [13][16]. A constant deceleration of 0.75g was applied to the vehicle to simulate braking at impact on a dry-asphalt surface. For a given impact configuration in the STS, the selected pedestrian model was configured into the corresponding gait stances and laterally struck from the left side by the relevant vehicle front (Figure 2) since about 80% of pedestrians were impacted from the lateral side in the GIDAS data.

According to a previous study, at low impact speeds (less than about 35 km/h) ground contact injuries are frequently the most severe injuries, while at higher impact speeds vehicle contact injuries are generally more severe [17]. To account for ground impacts while reducing the computing time, in this study the most serious injuries from either vehicle or ground contacts for low impact speed collisions ( $\leq 40$  km/h) were considered, but for higher impact speed cases ( $> 40$  km/h) only injuries from the vehicle contacts were considered by defining reasonable simulation time in the models.

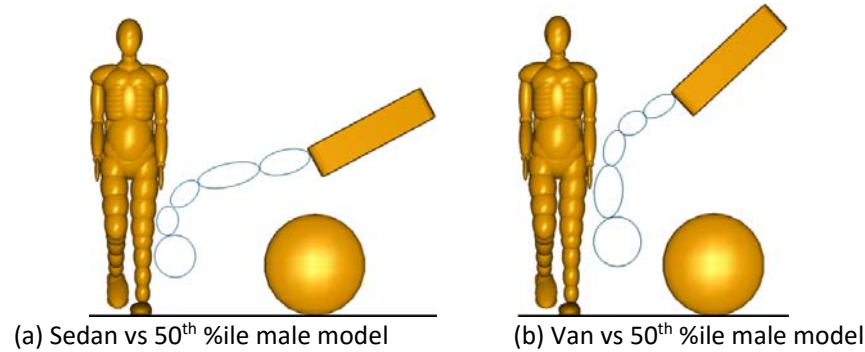


Fig. 2. Vehicle front models vs 50<sup>th</sup> %ile male model.

### ***Injury weighting system (IWS)***

Details of the IWS approach are available in [9]. Briefly, the AIS 2005 was used in the current study to classify predicted injuries [18]. According to previous studies on human body injury thresholds, the AIS level of an injury can be estimated from the predicted injury criteria scores for different body regions, which can be extracted from the MADYMO simulation outputs. Accordingly, predicted injuries from the multibody simulations were classified into AIS levels using injury criteria for the head (HIC), thorax (TTI), pelvis (lateral impact force), upper and lower legs (lateral bending moment) and knees (bending angle). The injury thresholds for these criteria for AIS score calculation were adapted from previous studies [11][19-21], see Table IV. The thresholds for upper and lower leg and pelvis AIS 2+ injuries were defined according to the pedestrian model size [11][21]. Based on the thresholds and injury parameters output from each impact simulation, the pedestrian Injury Number (IN) for a given collision was then calculated as the sum of all predicted AIS 2+ injuries from the above body regions of the struck pedestrian model. For example, the injury parameters output from an impact simulation for a 5<sup>th</sup> %ile female male model are: HIC-685, TTI-150 g, pelvis lateral impact force-8 kN, left upper leg lateral bending moment-300 Nm, right upper leg lateral bending moment-220 Nm, left knee lateral bending angle-17 degrees, right knee lateral bending angle-13 degrees, left lower leg lateral bending moment-260 Nm, right lower leg lateral bending moment-160 Nm, according to the thresholds (Table IV) the IN for this collision is 6 (head, thorax, pelvis, left upper leg, left knee and left lower leg). Due to the limitations of multi-body modelling and the injury criteria considered, only one injury was considered for each body region listed above.

TABLE IV  
INJURY CRITERIA FOR AIS 2+ INJURIES OF HEAD, THORAX, PELVIS AND LEG

<i>Body region/Injury criteria</i>	<i>Injury criteria level</i>	<i>Reference</i>
<i>Head/HIC</i>	$\geq 520$ (all models)	[21]
<i>Thorax/TTI (g)</i>	$\geq 100$ (all models)	[19]
<i>Pelvis/Lateral load (kN)</i>	$\geq 4.0$ -6.0 (adult)/1.0-2.0 (child)	[21]
<i>Upper leg/Bending moment (Nm)</i>	$\geq 55$ (3YOC)	[11]
	$\geq 140$ (6YOC)	
	$\geq 265$ (5th% female)	
<i>Knee/Bending angle (°)</i>	$\geq 350$ -575 (adult male)	[20]
	15 (all models)	
	$\geq 50$ (3YOC)	
<i>Lower leg/Bending moment (Nm)</i>	$\geq 85$ (6YOC)	[11]
	$\geq 240$ (5th% female)	
	$\geq 270$ -435 (adult male)	

To account for the distributions of each impact configuration, the involving proportion of the vehicle impact speed, pedestrian height and pedestrian gait stance used in the STS were applied to weight the predicted IN. Based on the distributions in Table I-III, the proportion of a given impact configuration ( $p_i$ ) in the STS is calculated as the product of the proportion of impact speed ( $p_{si}$ ), pedestrian height ( $p_{hi}$ ) and pedestrian gait stance ( $p_{gi}$ ), see Eq. (1). The sum of the proportions for each input parameter is unity, see Eq. (2) and Table I-III. Then the Weighted Injury Number (WIN) for the STS (size= $N$ ), is the sum of the product of the Injury Number ( $IN_i$ ) and the proportion ( $p_i$ ) for a given impact configuration in the STS, see Eq. (3). Thus the WIN score is the weighted average number of AIS 2+ injuries recorded per impact configuration in the STS. The WIN score, regarded as the resulting output of the VTS, can thus be used as a metric to distinguish the aggressivity of different vehicle front designs.

$$p_i = p_{si} * p_{hi} * p_{gi} \quad (1)$$

$$\sum_{i=1}^N p_i = \sum_{i=1}^N p_{si} = \sum_{i=1}^N p_{hi} = \sum_{i=1}^N p_{gi} = 1 \quad (2)$$

$$WIN = \sum_{i=1}^N IN_i * p_i \quad (3)$$

### Evaluation of VTS

To assess the capacity of the proposed VTS to predict the injury distributions observed in the GIDAS data, a Combined Injury Number (CIN) for AIS2+ injuries for the two vehicle classes was calculated from the individual WIN ( $WIN_{sed}$ -sedan and  $WIN_{van}$ -van) for each vehicle class and the frequency ( $p_{sed}$ -sedan = 94% and  $p_{van}$ -van = 6%) of occurrence of each vehicle class in the GIDAS, see Eq. (4). The sum of proportions for all vehicle classes is unity, see Eq. (5).

$$CIN = WIN_{sed} * p_{sed} + WIN_{van} * p_{van} \quad (4)$$

$$p_{sed} + p_{van} = 1 \quad (5)$$

To investigate the effects the number of impact configurations included in the STS on the injury predictive capacity of the VTS, combined injury numbers (CINs) were calculated for all the VTSs where different STSs were employed (Table A.I). Then comparisons of AIS 2+ injury distributions as a function of pedestrian body region and height, and vehicle class and impact speed, as well as the AIS 2+ injury rate (average AIS 2+ injury number for each collision) were conducted between these VTSs and the GIDAS data.

## III. RESULTS

Figures 3 and 4 show the predicted AIS 2+ distributions as a function of pedestrian body region and height, and vehicle impact speed and type between the CINs calculated from the WINs predicted by different sized VTSs. The GIDAS data are also shown as the reference. The proportions of AIS 2+ injuries to these five body regions and thirteen impact speeds from the GIDAS were normalised to keep a summation of 100% since injuries relating to other body parts and impact speeds were excluded in the simulation test sample. The comparisons conducted in Figure 3 and 4 were also 'normalized' to use the minimum number (three) of pedestrian height and impact speed groups considered in the VTSs. This avoids the exaggerated relative differences between the predicted injury proportions and the accident data for the VTSs where large numbers of pedestrian height and/or impact speed groups are used since for those cases the injury proportion of each group is very small.

Generally, the AIS 2+ injury distributions predicted from the VTSs are very similar to that in GIDAS data except those cases where very small STS samples were used, for example the VTS3-5-4/60, VTS-6-3-4/72, VTS-6-5-2/60 and VTS-3-3-2/18, see Figures 3 and 4. The differences in AIS 2+ injury distributions between VTSs using different STS sizes and GIDAS data are more evident for body region and impact speed than for pedestrian height and vehicle class. Figure 3 shows that the distribution of AIS 2+ injuries by body region for the GIDAS accident data and the VTSs are very similar. The head (about 30%) and leg (about 45%) are the dominant body regions for AIS 2+ injuries (Figure 3), which is also similar to the trend observed in the accident data from different countries [22]. For the comparison of AIS 2+ injury distribution as a function of pedestrian height, Figure 3 shows that the VTSs slightly over-predict the proportion of injuries associated with shorter individuals, and somewhat under-predict the proportions for midsize and taller pedestrians. These differences may be

partly because the impact locations were fixed in the central area of the vehicle front for the STS. A consequence of this is that the stiff A-pillar to head contact which can occur (especially for impacts away from the vehicle midline) for adult pedestrians is not represented in the VTS. In contrast, for children the head often contacts with the stiff bonnet leading edge area regardless of the pedestrian position with respect to the vehicle midline. This likely leads to the over-representation of the shorter pedestrians with respect to taller pedestrians in the VTSs observed in Figure 3.

The predicted distribution of AIS 2+ injury as a function of vehicle class shows good agreements with the GIDAS data, see Figure 4. However, the predicted injury frequencies at high impact speeds (>55km/h) are lower than that observed in the GIDAS accident data. This may be largely because of the simplification of impact scenarios and limitations in the modelling (contact, pedestrian model etc.). Another possible reason for this is that the injuries from ground impacts are not accounted for high impact speed cases, thus leading to under-predictions of injuries for the cases within the speed range.

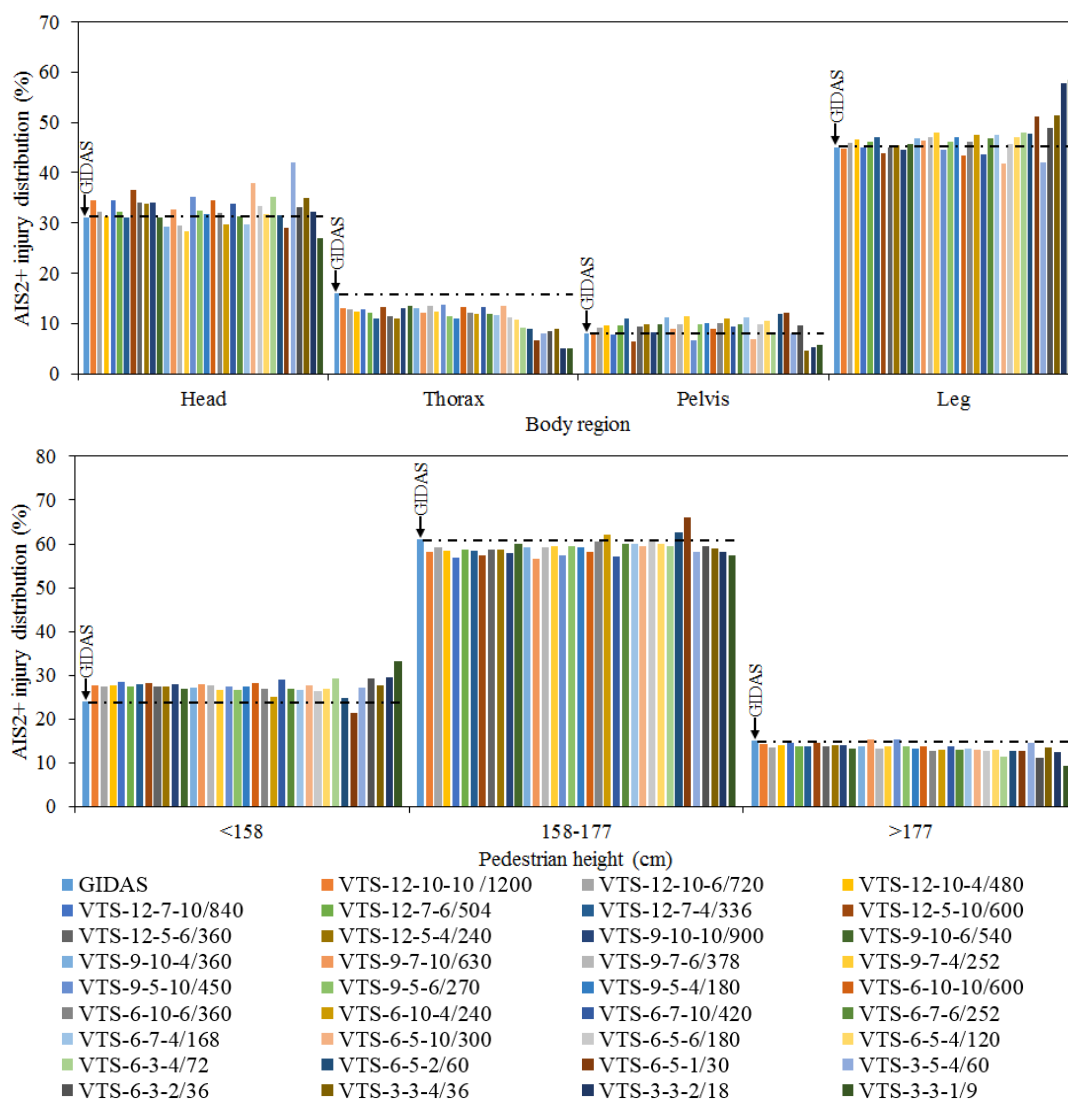


Fig. 3. Comparisons of AIS 2+ injury distributions as pedestrian body region and height between VTSs and GIDAS data.

Apart from the injury distributions, the normalised AIS 2+ injury number (injury rate) from the VTS and the GIDAS was compared in Figure 5. This shows the predicted AIS 2+ injury rates from VTSs using different STS sizes are very similar to that in GIDAS data except those cases where very small STS samples were used, for example the VTS3-5-4/60, VTS-6-3-4/72, VTS-6-5-2/60 and VTS-3-3-2/18. The predicted AIS 2+ injury rate is sensitive to the pedestrian gait stance, and the predicted AIS 2+ injury rate increases when decreasing the number of gait

stances included in the VTS. For example, the predicted AIS 2+ injury rate for VTS-6-5-2/60 (1.363) is obviously higher than that for VTS-6-5-4/120 (1.140), VTS-6-5-6/180 (1.081) and VTS-6-5-10/300 (1.042). This may be because that the high proportions of the gait stances with straight legs in the VTSs where less gait stances are used (Table III) raise the AIS 2+ injury rate in pedestrian legs (accounting for about 45% of all AIS 2+ injuries, see Figure 3), since the gait stances with straight legs have a higher injury risk to the leg than the flexed knees [6].

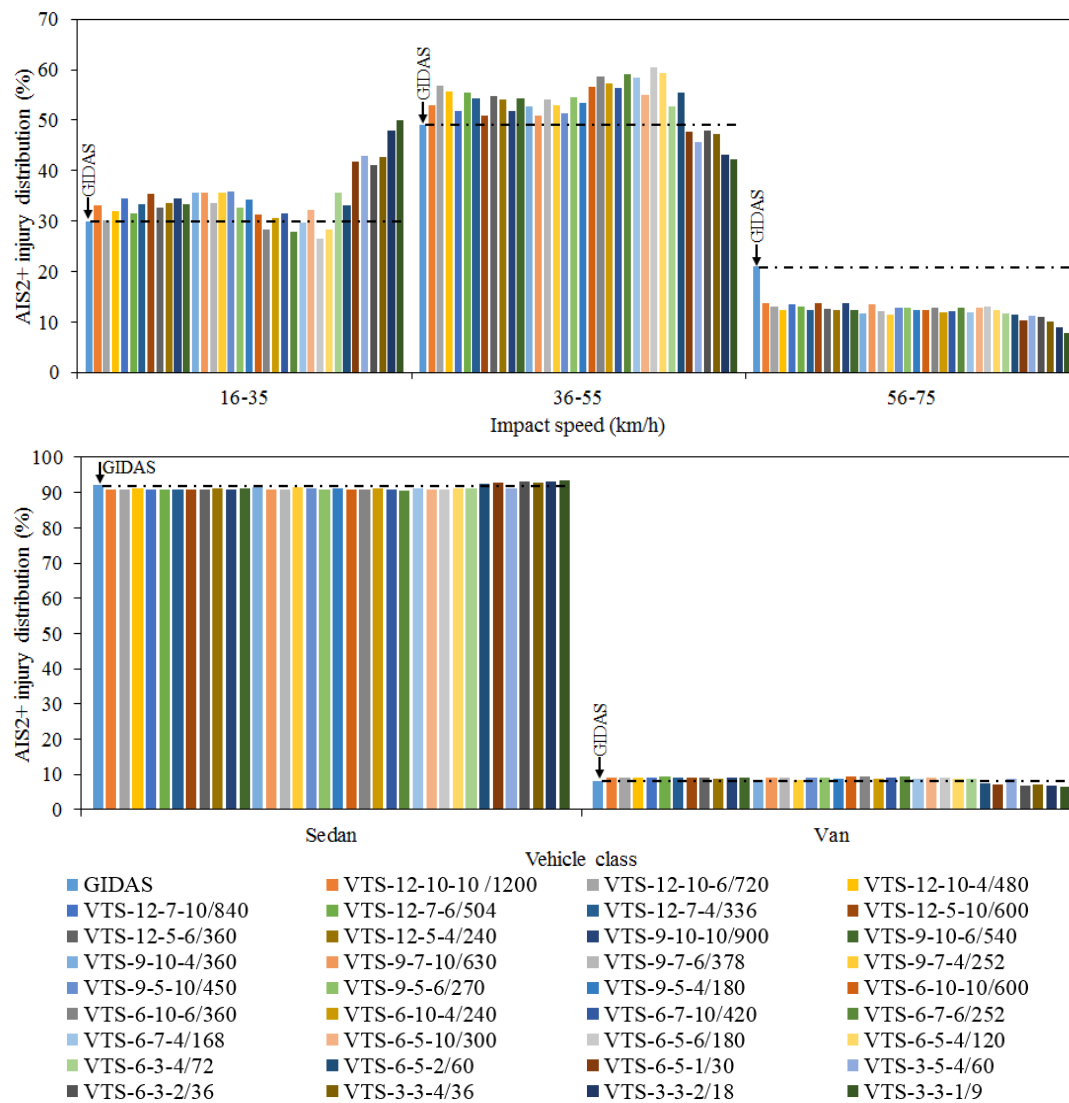


Fig. 4. Comparisons of AIS 2+ injury distributions as vehicle impact speed and class between VTSs and GIDAS data.



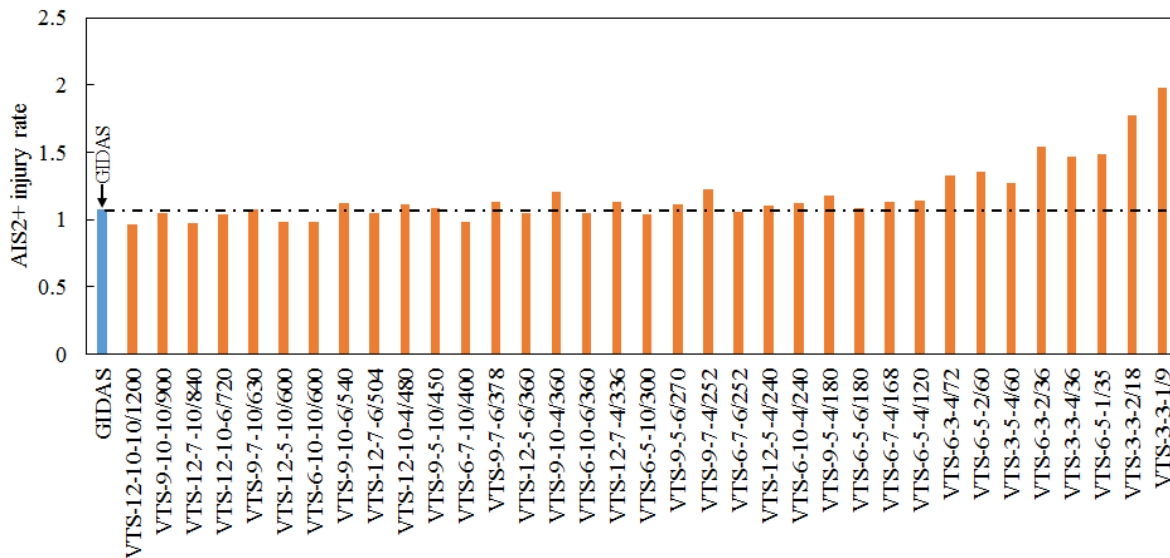


Fig. 5. Comparisons of AIS 2+ injury rate between VTs and GIDAS data.

Figure 6 shows the mean relative differences in AIS 2+ proportions for pedestrian body region and height, and vehicle impact speed and class between the CINs predicted by the VTs in different STS sizes and GIDAS data shown in Figure 3 and 4. The mean and standard deviation of relative error (with respect to the GIDAS data) of a VTs for a given distribution (body region, pedestrian height, impact speed and vehicle class) were calculated based on the relative differences of all the comparisons for a VTs in this distribution (i.e. for body region comparison, mean and standard deviation of the relative differences in AIS 2+ proportion for head, thorax, pelvis and leg). From this figure we can see that the sample size has visible effects on AIS 2+ injury distributions as a function of pedestrian body region and vehicle impact speed, but the effects for sample size on AIS 2+ injury distributions as pedestrian height and vehicle class are not so obvious. Figure 7 shows the relative errors in the AIS 2+ injury rate between the VTs using different STSs and GIDAS data. These comparisons help to reflect the representativeness of a VTs compared to the GIDAS accidents.

The results in Figures 6 and 7 indicate an obvious decrease in predictive capacity (relative error) with increasing the sample size when less than 120 impact configurations (red point) were employed in the STS. But the relative errors have no obvious reductions when a sample size bigger than 120 was applied.

The Wilcoxon test was applied to check the differences in the predicted relative errors shown in Figure 6 and 7 between the VTs using a STS size smaller than 120 and those VTs with a bigger STS size ( $\geq 120$ ). Table V shows the Wilcoxon test results, including the mean and standard deviation (SD) of the relative errors for VTs with a small or large STS size, and the significance level of the differences in the predicted relative errors. The Wilcoxon test results show that the predicted relative errors in AIS 2+ injury distribution as a function of body region and impact speed and the AIS 2+ injury rate for the VTs with a STS size smaller than 120 are significantly ( $p\text{-value} < 0.05$ ) higher than that for those VTs having a larger STS size ( $\geq 120$ ). The STS size is not significant ( $p\text{-value} > 0.05$ ) for the prediction of AIS 2+ injury distribution as a function of pedestrian height and vehicle class.

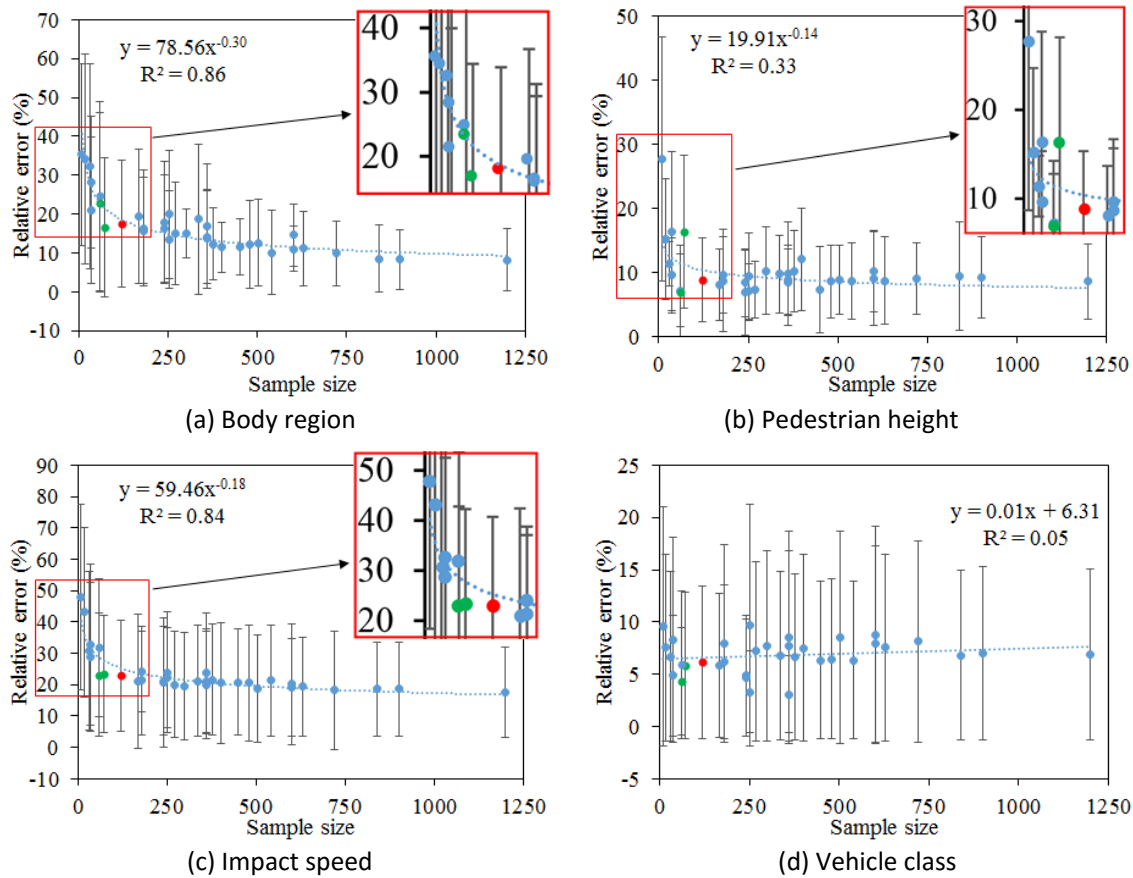


Fig. 6. Relative errors in AIS 2+ injury proportion as pedestrian body region and height, and vehicle impact speed and class between VTs and GIDAS data (120 at red point).

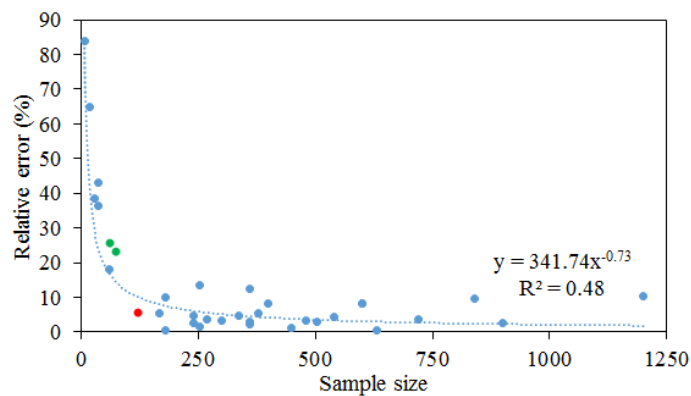


Fig. 7. Relative errors in AIS 2+ injury rate between VTs and GIDAS data (120 at red point).

TABLE V  
WILCOXON TEST RESULTS

AIS 2+ injury distribution/injury rate	STS size < 120		STS size ≥ 120		p-value
	Mean	SD	Mean	SD	
Body region	26.90	6.72	13.76	3.44	0.000
Pedestrian height	13.83	6.78	8.91	1.11	0.056
Impact speed	32.74	8.77	20.68	1.72	0.000
Vehicle class	6.64	1.77	6.83	1.54	0.603
Injury rate	41.68	22.42	5.28	3.61	0.000

Figure 8 shows the computational time (for a single vehicle model) as a function of the STS sample size for a given PC computer with parallel computing of four cores. The computational time (including the time for impact simulation and WIC calculation) increases in a reasonably linear manner with increase in the STS size. For the optimization work where a large number of vehicle designs need to be evaluated, a small STS sample size can substantially reduce the computational time.

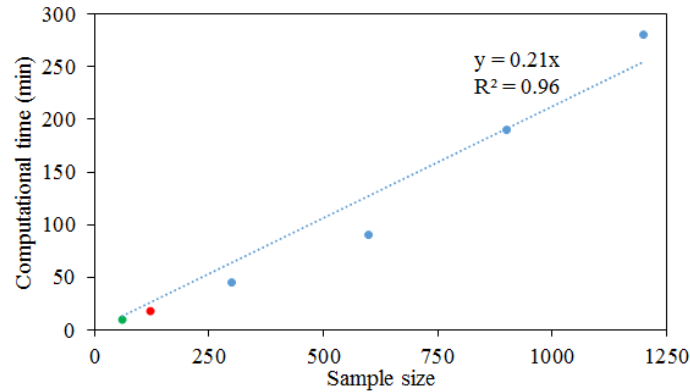


Fig. 8. Computational time as a function of STS sample size (120 at red point).

A linear regression model was used to establish the relationship between the mean relative errors in the predicted AIS 2+ injury distribution as a function of body region and impact speed (Figure 6 (a) and (c)), as well as the relative error in the predicted AIS 2+ injury rate (Figure 7) and the number of impact parameter groups used in the STS. The model is:

$$REs = C + B_s * N_s + B_h * N_h + B_g * N_g, \quad (6)$$

where the  $REs$  are the predicted relative errors for a given comparison described above,  $C$  is the constant of the regression model,  $B$  and  $N$  are the coefficient and number of group for each impact parameter, respectively. The subscripts in Eq. (6) are the impact speed ( $s$ ), pedestrian height ( $h$ ) and gait stance ( $g$ ). Table VI shows the regression analysis results. The R-square values (0.48-0.79), which are the coefficients of determination of the regression models reflecting the correlation between the input data (relative errors) and that estimated from the regression functions, indicate that the regression models can generally represent the relationships between the numbers of impact parameters and the predicted relative errors. Table VI also shows the coefficients and p-values for these impact parameters in each comparison, where the coefficient reflects the importance and significance level of the corresponding impact parameter in the regression. It is clear that three impact parameters are statistically significant ( $p\text{-value} < 0.05$ ) for the predicted relative errors of AIS 2+ injury distribution as a function of body region and impact speed. The negative coefficients for all of these impact parameters indicate that the relative error decreases with increasing the number of groups of impact speed, pedestrian height and gait stance used in the STS. For the prediction of AIS 2+ injury distribution as body region in GIDAS, the pedestrian gait stance (-1.10) is more important than the impact speed (-0.68) and pedestrian height (-0.76). The impact speed is the most importance factor influence the prediction of AIS 2+ injury distribution as a function of impact speed in GIDAS. For the prediction of AIS 2+ injury rate in GIDAS, the effect of pedestrian height is more significant.

TABLE VI  
REGRESSION ANALYSIS RESULTS

<i>Relative error (RE)</i>	Impact parameter	Constant	B	R-square	p-value
<i>Body region</i>	Impact speed	33.00	-0.68	0.79	0.001
	Pedestrian height		-0.76		0.002
	Gait stance group		-1.10		0.000
<i>Impact speed</i>	Speed group	36.53	-0.82	0.64	0.001
	Height group		-0.53		0.047
	Gait stance group		-0.64		0.007
<i>Injury rate</i>	Speed group	44.25	-1.49	0.48	0.042
	Height group		-1.81		0.044
	Gait stance group		-1.54		0.045

According to the above analysis, a sample size of 120 (VTS-6-5-4/120) is a good choice based on the current selected impact configurations and numerical methods since it covers broad ranges of impact speed (six groups from 16 to 75 km/h), pedestrian height (five sizes from child to large adult male) and pedestrian gait stance (straight or flexed and forward or backward), and this sample has a reasonable predictive capacity for injuries (mean relative error of 17.6%, 8.8%, 22.8% and 6.1% for AIS 2+ distribution as a function of body region, pedestrian height, vehicle impact speed and vehicle class comparisons respectively, and 5.9% for AIS 2+ injury rate comparison) compared to real-world accidents, see Figure 6 and 7 (red point). Furthermore, the VTS of 120 simulations is much more computationally efficient than those cases having a bigger STS size (Figure 8) for future vehicle front optimisation for pedestrian protection, where many vehicle design variables need to be taken into consideration. The results from Figure 3-7 indicate that the VTSs which have a STS size of 60 (VTS-6-5-2/60) or 72 (VTS-6-3-4/72) and use at least six impact speed bins can predict the AIS 2+ injury distributions and AIS 2+ injury rate observed from GIDAS data with mean relative errors less than 25% (green points in Figure 6 and 7). These VTSs are also options for assessing pedestrian safety performance of vehicle front designs in future optimisation.

#### IV. DISCUSSION

##### **Strengths**

The results of the current study indicate that the AIS 2+ injury distribution and AIS 2+ injury rate of pedestrians predicted from the VTS considering a reasonable range of impact configurations show good matches with that observed from GIDAS data when the same vehicle class distribution as the accident data is employed to the VTS. This is a strong support to the findings of our previous study where the PCDS data were compared [9]. These results, together with those reported in [9] suggest that it is reliable to use the VTS for assessing the pedestrian safety performance of vehicle front designs at a general level.

This study also indicates that the injury predictive capability of the VTS does not always significantly increase with increasing the STS size and the effects of sample size are small when the STS size achieves a reasonable value (i.e. around 120), see Figure 6 and 7. The results suggest that it is better to use at least six impact speed cases in the STS. The benefit of using a reasonable STS size for assessing vehicle front safety performance is to control the computational time when considering a range of impact configurations. Therefore users can define the VTS according to the impact configurations which need to be tested and their computational time limits. The STS and IWS approaches proposed in the current study can also be applied in automotive industry in terms of evaluating new car pedestrian safety performance with a consideration of a broad range of impact configurations rather than only using limited conditions. Detailed analysis of real accidents using video evidence can help with this.

##### **Limitations**

Although the modelling presented here is broadly representative of the range of real-world pedestrian collisions, pedestrian accidents are complex events which cannot be fully modelled. The VTS is based on simulations using simplified vehicle and pedestrian models, and the limitations of multi-body modelling (e.g. contact, injury prediction, etc.) influence the injury predictive capability of the VTS. The different pedestrian

sizes were obtained by scaling the mid-size male model and have not been explicitly validated. Only one injury was accounted for in each body part in the VTS, including injuries to the head, neck, chest, pelvis, femur (left and right), knee (left and right) and tibia (left and right). The multi-injury condition of bone fractures accompanied by damage to the internal organs cannot currently be predicted by the multi-body pedestrian model, and the effects of gender, age and weight on anthropometry and injury criteria thresholds have not been accounted for. Only one vehicle model was used to represent the range of shapes within a vehicle class. The variations of initial impact location on the vehicle front and the detailed shapes and stiffness of the vehicle front structures have also not been considered in the simulations. Pedestrian ground contact injuries for cases at high impact speeds (>40 km/h) were not accounted for but the injuries from the ground contacts may increase the predicted WIN score and head injury proportion for the van.

The predicted injury distribution and injury rate are influenced by the variation of the vehicle model (shape and stiffness) [9], impact condition (impact angle et al.), pedestrian model (knee height, pelvis height, weight, mechanical characteristics et al.) and injury criteria and thresholds. For example, using a higher bonnet leading edge car model would increase pelvis injury proportion and using stiffer contact characteristics would increase the injury rate. In summary, the proposed VTS and the evaluation of its injury predictive capability are only at the generalised level. The results of this study are therefore mainly for having a basic understanding on the selection of impact configurations which will be considered in our future optimization of vehicle front design for pedestrian protection.

## V. CONCLUSIONS

The generalised predictive capability of the proposed Virtual Test Sample (VTS) for assessing pedestrian injury distributions accounting for different impact configurations was evaluated by comparing AIS 2+ injury distributions as a function of different pedestrian body regions and height groups, vehicle classes and impact speeds, as well as the AIS 2+ injury rate between the VTSs and the GIDAS accident data. The results indicate that the proposed VTS using a reasonable STS (120 impact configurations or more) is broadly capable of predicting the AIS 2+ injury rate and distribution of pedestrian AIS 2+ injuries observed from the real-world accidents when the same vehicle class distribution as the accident data is employed. The VTS can be considered as an effective approach for assessing pedestrian safety performance of vehicle front designs at the generalised level.

## VI. ACKNOWLEDGEMENT

The authors gratefully thank Tom Daniel, Dan Larner and Atul Gupta from Google for advice on impact scenario selection, and the supports from China Scholarship Council.

## VII. REFERENCES

- [1] World Bank Group. "Road Safety", Internet: [<http://www.worldbank.org/transport/roads/safety.htm>], Date accessed December 5, 2013.
- [2] Simms CK, Wood DP. Pedestrian and cyclist impact. *Springer*, London, UK, 2009.
- [3] CNCAP. *The protection for pedestrians in the event of a collision*. China New Car Assessment Programme, 2015.
- [4] EEVC. *Improved test methods to evaluate pedestrian protection affordable by passenger cars, technical report*. European Enhanced Vehicle-safety Committee; EEVC Working Group17 Report, December 1998 with September 2002 updates, 2002.
- [5] EuroNCAP. *Pedestrian Testing Protocol*. European New Car Assessment Programme, 2013.
- [6] Li G, Yang J, Simms C. The influence of gait stance on pedestrian lower limb injury risk. *Accident Analysis & Prevention*, 2015, **85**:83-92.
- [7] Peng Y, Deck C, Yang J, Willinger R. Effects of pedestrian gait, vehicle-front geometry and impact velocity on kinematics of adult and child pedestrian head. *International Journal of Crashworthiness*, 2012, **17**(5):553-561.
- [8] Elliott J, Simms C, Wood D. Pedestrian head translation, rotation and impact velocity: The influence of vehicle speed, pedestrian speed and pedestrian gait. *Accident Analysis & Prevention*, 2012, **45**:342-353.
- [9] Li G, Yang J, Simms C. A virtual test system representing the distribution of pedestrian impact configurations for future vehicle front-end optimization. *Traffic Injury Prevention*, 2016 (in press), DOI:10.1080/15389588.2015.1120294.

- [10] Li G, Otte D, Yang J, Simms C. Pedestrian injury trends evaluated by comparison of the PCDS and GIDAS databases. *Proceedings of the IRCOBI Asia Conference*, 2016, Seoul, South Korea.
- [11] MADYMO. *Human Body Models Manual Release 7.4.1*. TNO, 2012.
- [12] Untaroiu CD, Meissner MU, Crandall JR, Takahashi Y, Okamoto M, Ito O. Crash reconstruction of pedestrian accidents using optimization techniques. *International Journal of Impact Engineering*, 2009, **36**(2):210-219.
- [13] Crocetta G, Piantini S, Pierini M, Simms C. The influence of vehicle front-end design on pedestrian ground impact. *Accident Analysis & Prevention*, 2015, **79**:56-69.
- [14] Martinez L, Guerra LJ, Ferichola G, Garcia A, Yang J. Stiffness corridors of the European fleet for pedestrian simulation. *Proceedings of the International Technical Conference on the Enhanced Safety of Vehicles*. 2007, Lyon, France.
- [15] Mizuno K, Kajzer J. Compatibility problems in frontal, side, single car collisions and car-to-pedestrian accidents in Japan. *Accident Analysis & Prevention*, 1999, **31**(4):381-391.
- [16] Lyons M, Simms C. Predicting the influence of windscreen design on pedestrian head injuries. *Proceedings of the IRCOBI Conference*, 2012, Dublin, Ireland.
- [17] Guillaume A, Hermitte T, Hervé V, Fricheteau R. Car or ground: which causes more pedestrian injuries? *Proceedings of the International Technical Conference on the Enhanced Safety of Vehicles*, 2015, Gothenburg, Sweden.
- [18] Gennarelli TA, Wodzin E. AIS 2005: a contemporary injury scale. *Injury*, 2006, **37**(12):1083-1091.
- [19] Cavanaugh JM, Zhu Y, Huang Y, King AI. Injury and response of the thorax in side impact cadaveric tests. *SAE Technical Paper No.933127*, 1993.
- [20] Mo F, Arnoux PJ, Cesari D, Masson C. Investigation of the injury threshold of knee ligaments by the parametric study of car-pedestrian impact conditions. *Safety Science*, 2014, **62**:58-67.
- [21] Payne AR, Patel S, "OPERAS Project 427519", Internet [<http://www.eurailsafe.net/subsites/operas>], MIRA, 2001, Date accessed May 12, 2014.
- [22] Hu J, Klinich KD. Toward designing pedestrian-friendly vehicles. Michigan: The University of Michigan Transportation Research Institute, *Report No. UMTRI-2012-19*, 2012, pp.4-5.

## VIII. APPENDIX

TABLE A.I

INFORMATION OF VTSS WITH DIFFERENT STS SIZES (IMPACT SCENARIOS)

Test	<i>VTs name</i>	Number of speed bin	Number of pedestrian height bin	Number of pedestrian gait stance bin	Number of impact scenario
1	<i>VTs-12-10-10/1200</i>	12	10	10	1200
2	<i>VTs-12-10-6/720</i>	12	10	6	720
3	<i>VTs-12-10-4/480</i>	12	10	4	480
4	<i>VTs-12-7-10/840</i>	12	7	10	840
5	<i>VTs-12-7-6/504</i>	12	7	6	504
6	<i>VTs-12-7-4/336</i>	12	7	4	336
7	<i>VTs-12-5-10/600</i>	12	5	10	660
8	<i>VTs-12-5-6/360</i>	12	5	6	360
9	<i>VTs-12-5-4/240</i>	12	5	4	240
10	<i>VTs-9-10-10/900</i>	9	10	10	900
11	<i>VTs-9-10-6/540</i>	9	10	6	540
12	<i>VTs-9-10-4/360</i>	9	10	4	360
13	<i>VTs-9-7-10/630</i>	9	7	10	630
14	<i>VTs-9-7-6/378</i>	9	7	6	378
15	<i>VTs-9-7-4/252</i>	9	7	4	252
16	<i>VTs-9-5-10/450</i>	9	5	10	450
17	<i>VTs-9-5-6/270</i>	9	5	6	270
18	<i>VTs-9-5-4/180</i>	9	5	4	180
19	<i>VTs-6-10-10/600</i>	6	10	10	600
20	<i>VTs-6-10-6/360</i>	6	10	6	360
21	<i>VTs-6-10-4/240</i>	6	10	4	240
22	<i>VTs-6-7-10/420</i>	6	7	10	420
23	<i>VTs-6-7-6/252</i>	6	7	6	252
24	<i>VTs-6-7-4/168</i>	6	7	4	168
25	<i>VTs-6-5-10/300</i>	6	5	10	300
26	<i>VTs-6-5-6/180</i>	6	5	6	180
27	<i>VTs-6-5-4/120</i>	6	5	4	120
28	<i>VTs-6-3-4/72</i>	6	3	4	72
29	<i>VTs-6-5-2/60</i>	6	5	2	60
30	<i>VTs-6-5-1/30</i>	6	5	1	30
31	<i>VTs-6-3-2/36</i>	6	3	2	36
32	<i>VTs-3-5-4/60</i>	3	5	4	60
33	<i>VTs-3-3-4/36</i>	3	3	4	36
34	<i>VTs-3-3-2/18</i>	3	3	2	18
35	<i>VTs-3-3-1/9</i>	3	3	1	9